P.O.Box 2345, Beijing 100023,China
Fax: +86-10-85381893
E-mail: wcjd@public.bta.net.cn www.wjgnet.com

World J Gastroenterol 2002;8(6):1035-1039
World Journal of Gastroenterology
 ISSN 1007-9327

• LIVER CANCER •

An implantable rat liver tumor model for experimental transarterial chemoembolization therapy and its imaging features

Xin Li, Chuan-Sheng Zheng, Gan-Sheng Feng, Chen-Kai Zhuo, Jun-Gong Zhao, Xi Liu

Xin Li, Chuan-Sheng Zheng, Gan-Sheng Feng, Chen-Kai Zhuo, Jun-Gong Zhao, Xi Liu, Department of Interventional Radiology, Union Hospital, Tongji Medical College, Huazhong University of Science and Technology, Wuhan 430022, Hubei Province, China
Supported by the National Natural Science Foundation of China, No.39770839
Correspondence to: Dr. Xin Li, Department of Interventional Radiology, Union Hospital, Tongji Medical College, Huazhong University of Science and Technology, Wuhan 430022, Hubei Province, China. wxyao2001@yahoo.com.cn
Telephone: +86-27-85726432
Received 2002-07-04 **Accepted** 2002-07-25

Abstract

AIM: To establish an ideal implantable rat liver tumor model for interventional therapy study and examine its angiographic signs and MRI, CT features before and after embolization.

METHODS: Forty male Wistar rats were implanted with Walker-256 tumor in the left lateral lobe of liver. Digital subtraction angiography (DSA) and transarterial chemoembolization were performed on day 14 after implantation. Native computer tomography (CT, n=8) and native magnetic resonance (MR, n=40) were performed between the day 8 and day 21 after implantation. The radiological morphological characteristics were correlated with histological findings.

RESULTS: Successful implantation was achieved in all forty rats, which was confirmed by CT and MRI. MR allowed tumor visualization from day 8 while CT from day 11 after implantation. The tumors were hypodensity on CT, hypointense on MR T1-weighted and hyperintense on T2-weighted. The model closely resembled human hepatocarcinoma in growth pattern and the lesions were rich in vasculature on angiography and got its filling mainly from the hepatic artery. Before therapy, tumor size was 211.9±48.7 mm^3. No ascites, satellite liver nodules or lung metastasis were found. One week after therapy, tumor size was 963.6±214.8 mm^3 in the control group and 356.5±78.4mm^3 in TACE group. Ascites (4/40), satellite liver nodules (7 /40) or lung metastasis (3 /40) could be seen on day 21.

CONCLUSION: Walker-256 tumor rat model is suitable for the interventional experiment. CT and MRI are helpful in animal optioning and evaluating experimental results.

Li X, Zheng CS, Feng GS, Zhuo CK, Zhao JG, Liu X. An implantable rat liver tumor model for experimental transarterial chemoembolization therapy and its imaging features. *World J Gastroenterol* 2002; 8(6):1035-1039

INTRODUCTION

Hepatocellular carcinoma (HCC) is a relatively common malignant tumor and its prognosis is poor[1,2]. The first choice of treatment is hepatectomy, but most cases are considered inoperable due to extreme tumor extension at the time of diagnosis and/or accompanying advanced cirrhosis[2,3]. Moreover, it will respond neither to radiotherapy nor to systemic chemotherapy, the most frequently applied palliative treatment option for locally advanced tumors is transarterial chemoembolization (TACE)[3-7]. Various protocols have been proposed with different chemotherapeutic agent, different embolization materials and different approaches. Lack of carefully designed, prospective and randomized trials has caused the most suitable scheme of TACE not yet established[8]. In order to accelerate the study of TACE strategies for HCC, it is necessary to have a suitable and reproducible animal model.

The aim of the present study was to establish an implantable rat liver tumor model for experimental TACE therapy, and deliberate its angiographic signs and MRI, CT features before and after TACE.

MATERIALS AND METHODS

Tumor and animals

The Walker-256 carcinosarcoma cell line was obtained from the Cell Preservation Center of Wuhan University (Wuhan, Hubei, P. R. China). Forty male Wistar rats weighing 200±20 g (experiment animal center, Tongji Medical College, Huazhong University of Science and Technology) were used.

Tumor implantation

Tumor implantation was performed using a modification of the technique described by Yang *et al*[9]. A 2-week-old subcutaneously growing solid tumor was explanted from a donor animal and minced into small cubes of about 2 mm^3. The recipient animals were laparotomized through a midline abdominal incision under intraperitoneal anesthesia with 1 % pentobarbitale sodium (30 mg/ kg body weight). The left lateral lobe of the liver was protruded out of the abdominal cavity and a subcapsular tunnel about 3-5 mm depth was made by a fine-point tweezer. Then a solid tumor fragment was inserted into the subcapsular tunnel and fixed with a small piece of gelfoam on the liver surface. No hemostasis was necessary.

Catheterization of the hepatic artery

14 days after the implantation, a second laparotomy was performed for angiographic studies and TACE therapy[10]. Another midline abdominal incision was performed under the general anesthesia. The common hepatic artery, the gastroduodenal artery and the right hepatic artery were isolated using a binocular operative microscope (Suzhou Medical Instruments Factory, Jiansu, China). Through an arteriotomy of the gastroduodenal artery, a polyethylene catheter (0.3 mm in inside diameter and 0.5 mm in outside diameter) was inserted retrogradely into the gastroduodenal artery and temporarily fixed by a suture.

Animal group and drugs doses

Forty rats were randomly divided into two groups (Control

group and TACE group) of twenty rats each. Control group received 0.3 ml normal saline and TACE group received 0.5 ml / kg of iodized oil (Lipiodol UltraFluid, Andre Guerbet, Aulnay-sous-Bois, France) which were given by slow retrograded manual injected into the gastroduodenal artery while the common hepatic artery and right hepatic artery were temporarily ligated.

Imaging

Hepatic artery angiography was performed by using a digital angiographic unit (Bicor Top, Siemens, Germany). A 0.3 ml bolus of contrast medium (300 mg iodine/ml, Ultravist 300, Schering, Germany) was manually injected retrogradely via the surgically implanted catheter into the gastroduodenal artery. CT (n=8) and MR imaging (n=40) were performed at 8, 11, 14 days after the implantation and 7 or 8 days after the angiography and TACE therapy. Animals were anesthetized as described earlier prior to imaging. CT scans were performed on Somatom Plus 4 spiral Scanner (Siemens, Germany) with 3.0 mm scan thickness and 3.0 increments (pitch=1.0), a field of view of 150 mm, 140 mA and 80kVp. Documentation was performed with a window width of 250 and a center of 50 Hounsfield units. MR images were performed on 1.5-Tesla system (Siemens Vision, Siemens, Germany) supplemented by a cervical coil. T1-weighted (TR/TE, 450/12 msec) and T2-weighted (TR/TE, 2800/96 msec) transverse SE images (slice thickness 2mm) were acquired using acquisition times of 7:25 and 6:16 min, respectively.

Tumor volume was determined from MR measurements of the largest and smallest diameter and calculated according to the following formula: Tumor volume (mm^3)=largest diameter (mm)×[smallest diameter (mm)]^2/2.

Histologic evaluation

Forty rats were sacrificed at 2 (ten rats) and 7 (thirty rats) days after TACE, respectively. Samples of liver tumors were fixed in 10 % formalin, dehydrated and embedded in paraffin; 5-μm sections were stained with hematoxylin-eosin for light microscopy and measurement of the degree of tumor necrosis.

RESULTS

Tumor uptake, Tumor growth, and Histopathological findings

Tumor implantation led to the outgrowth of liver tumor nodules in all forty rats. The lesions were located in the left lobe of the liver as a solitary mass. Mean volume of the tumor measured by MR examination was 211.9±48.7 mm^3 14 days after implantation, there was no statistic difference between the control and the TACE groups. No ascites, satellite liver nodules or lung metastasis was found. One week after therapy, mean volume of the tumor were 963.6±214.8 mm^3 in the control group and 356.5±78.4 mm^3 in TACE group and there were significant statistic differences between them (t=8.396, P<0.001). Ascites (4/40), satellite liver nodules (7/40) or lung metastasis (3/40) could be seen in some models at day 21.

Hematoxylin-eosin (H & E) stained sections of the liver specimens showed a poorly differentiated carcinoma, which were usually roughly spherical or ovoid in shape. Tumor cells arranged in irregular groups and the signs of malignancy, including hyperchromatosis, polymorphism and numerous mitoses were detected. The mass had a sharp demarcation from the surrounding normal hepatic parenchyma; its capsules were thin and composed of collagen fibers, which were caused by the compression of the tumor. The tumor showed inhomogeneous signs of hypervascularization consisting mainly of small arteries and capillaries. Satellite nodules or portal vein tumor embolization could be seen in some models (Figure 1).

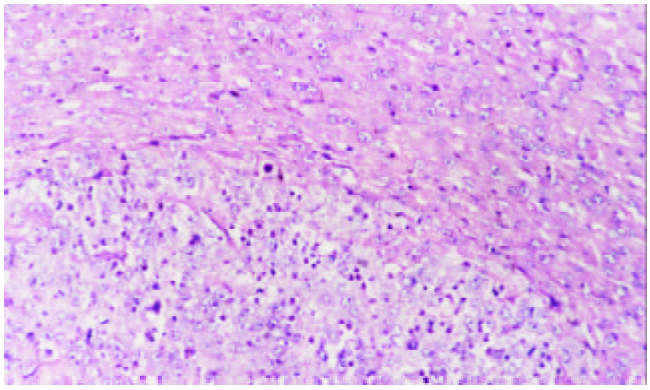

Figure 1 Control group, 7 days after hepatic artery infusion, show tumor and thin capsule. Hematoxylin-eosin ×200

Spontaneous spotty, scattered necrosis were seen in all cases of the control group 7 days after the therapy. 2 days after iodized oil embolization, the range of tumor central necrosis obviously enlarged to moderate (16/20) or even severe degree (4/20). Intra-tumor hemorrhage and bile stasis were seen in some cases. Tumor cells tended to remain viable in the periphery of nodules in the samples 7 days after embolization. We also found thick fibrous capsules around the tumor with chronic inflammation and granulomatosis. Different degree of degeneration or necrosis were seen in normal hepatic parenchyma adjacent the tumor (Figure 2).

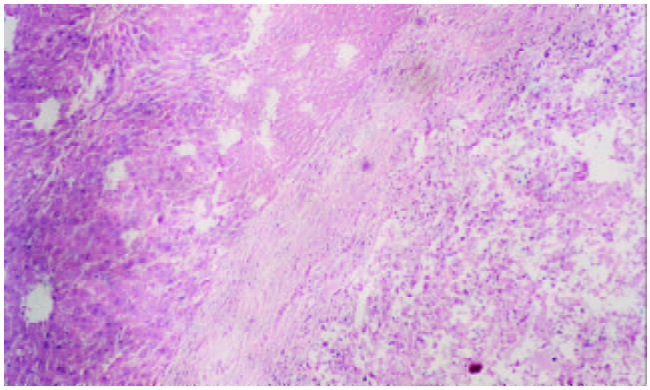

Figure 2 TACE group, 7 days after hepatic artery embolization, show tumor center necrosis, thick fibrous capsules, and degeneration or necrosis in normal hepatic parenchyma adjacent the tumor. Hematoxylin-eosin ×100.

Tumor imaging

8 days after the implantation, MR could show node with clear shape in some cases, which showed hypointensity on T1-weighted and hyperintensity on T2-weighted (Figure 3). 14 days after the implantation, MR could detect lesions in all cases. Some degree of necrosis was seen in the center of the mass in 17 cases, presented as a lower intensity on T1 and T2-weighted as compared with the pathologic tissue without necrosis (Figure 4).

One week after hepatic artery infusions, necrosis was found in all cases of control group and little change was found before and after therapy. While in TACE group, MR features were as follows: the signal in the center of lesion was asymmetrical

and mixed (high, intermediate, and low) on T2-weighted. Rim sign with varying thickness of slight high signal intensity was seen on T1 and T2-weighted (Figure 5). In addition, the presence of ascites, satellite liver nodules or lung metastasis could be shown well on MR imaging.

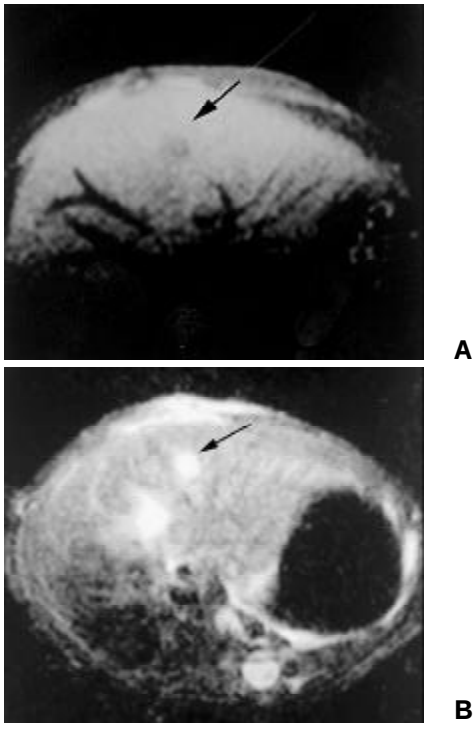

Figure 3 8 days after the implantation, MR demonstrate a node with clear shape, hypointensity on T1- weighted (A) and hyperintensity on T2 – weighted (B)

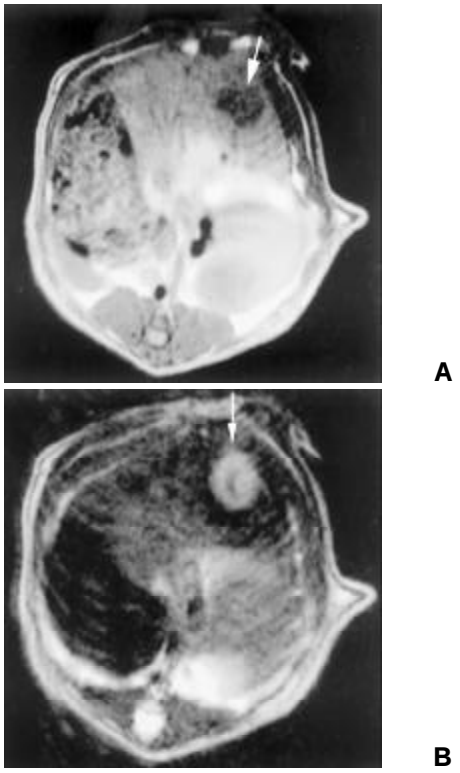

Figure 4 14 days after the implantation, tumor center showed lower intensity on T1 (A) and T2-weighted (B) than that of periphery, which indicate coagulation necrosis

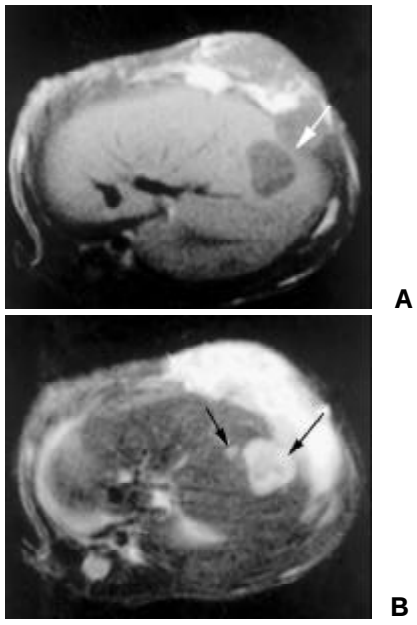

Figure 5 One week after TACE, MR showed center necrosis, periphery rim sign of slight higher T1 (A) and T2 (B) intensity, and the satellite nodular (B)

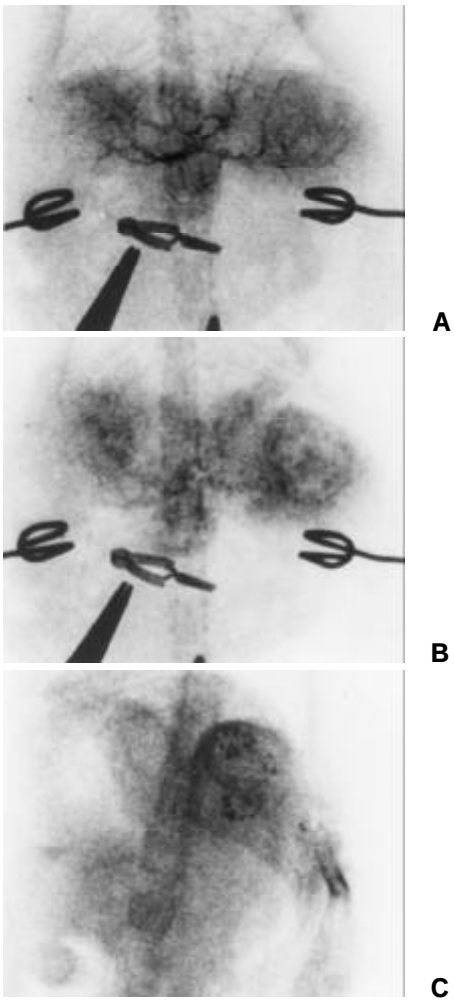

Figure 6 The tumor were mainly fed by the hepatic artery. Angiography features including hypervascularity, irregular tortuous and convoluted vessels (A), tumor stain (B) and the deposition of iodized oil in tumor after embolization (C)

Tumor could first be identified at day 11 after implantation on native CT. CT depicted the tumor as hypodensity masses and well discernible from the surrounding liver tissues. Some lesions were less dense in the central areas. After TACE, CT scans showed the dense deposition of iodized oil in tumor.

The hepatic artery mainly fed the tumors. Angiographic features included neovascularity, hypervascularity, irregular tortuous and convoluted vessels, tumor stain and sometime with contrast puddling. But no arterivenous shunts or early venous drainage were seen. Those with central necrosis showed a contrast-enhancing periphery and a nonenhancing center. After embolization, main branches of the left hepatic artery were occluded and the deposition of iodized oil in tumor could be seen (Figure 6).

Comparative study of image and pathologic findings

The clear border shown by MR represented the fiber septum caused by the compression of the tumor on neighboring normal liver tissue. Central areas of lower density in CT, lower signal intensity on T1-weighted images and T2-weighted images were compatible with central necrosis. After therapy, central areas of high signal intensity on T2-weighted images correlated with areas of liquefaction necrosis, which were more common in larger lesion. Areas of low or intermediate signal intensity of the lesion on T2-weighted images corresponded to coagulation necrosis. The peripheral rim with varying thickness of slight high signal intensity on T1 and T2-weighted images correlated with the thick fibrous capsules and the granulation tissues.

DISCUSSION

TACE has been widely carried out and is considered an effective treatment for HCC patients who are not candidates for surgery[3-8]. But as to selection of patient, TACE approaches and therapeutic efficacy, there were great variation by the different studies reported to date[5,11-13]. Standardization of proper patient selection and choice of optimal TACE methods selection remain to be determined, which severely embarrass the further progress of TACE in HCC therapy. Many scholars advocate prospective randomized controlled trials to assess the efficacy of different TACE strategies[8,14,15]. But the reaction to TACE is influenced by many factors, such as tumor differentiation, size, blood supply, liver function and adverse effect to the treatment make it difficult to judge the real efficacy of a certain TACE regime[16-21]. Replication a suitable animol model for TACE therapy can overcome these shortages. We can study the efficacy of TACE on tumor of same differentiation and similar size, location and number. Experiments on tumor model will help in exploring new technique of TACE, studying the effectiveness of different therapeutic strategies and evaluating TACE related adverse effect.

Various methods have been introduced to develop intrahepatic tumor models. Nude rats transplantation models are relatively hard to feed, need more complicate manipulation in tumor implantation and hepatic artery therapy and were more expensive[22-24]. Induction with hepatocarcinogens (such as diethylnitrosamine or aflatoxin) will produce multifocal liver tumors[25,26]. Many implantation tumors (such us Novikoff hepatoma or DHD K12 colon carcinoma cells) show early central necrosis, early systemic metastasis, or appear hypovascular[27-29]. All of these models were not suitable for TACE study. In the present study we establish Walker-256 transplanted liver tumor model and examine its tumor growth characteristic, blood supply and imaging features to judge the potential of this model in the experimental study of TACE[30].

The models show reproducibility on tumor growth rate and growth characteristic. The lesions get it' s blood supply mainly from hepatic artery, rich in vasculature and had similar angiographic features similar to that of HCC[31,32]. We concluded the tumor around 14 days after implantation was suitable for TACE experimental study-by the time the tumor had proper size, hypervascularization and no evident central necrosis.

Imaging procedures allowed monitoring of tumor size at the time of intervention and during the follow-up period without sacrificing animal and thus reduced the number of animals needed. In this series, we investigated the visualization and sizing of tumors using native CT and MR, which had been proven very useful for the clinical assessment of the effects of TACE in HCC[33-35]. The CT and MR appearance of Walker-256 carcinoma before and after TACE is similar to that of HCC in humans. It can reflect the histopathologic changes in some degree and determine the treatment efficacy preliminarily. We found MR is superior to CT in tumor detection. In further studies, MR and CT features before and after contrast media administration will be carried out to obtain further information[36-38].

The left lateral lobe is the largest one in many rat liver lobes and the left hepatic artery has a larger caliber than the right one. So we chose the left lateral lobe as the target during the tumor implantation. After the liver was returned to the abdominal cavity, the implantation site was spontaneous covered by parts of the median lobe. Simultaneously, we fixed the tumor fragment with a small piece of gelfoam on the liver surface. Our implantation techniques guaranteed the intra-parenchyma tumor growth and avoided the artificial technique -induced tumor dissemination.

According to our trial experiment and literature, the iodized oil dosage chosen for embolization was 0.5 ml / kg, which can obstruct the secondary branches of the left hepatic artery[39]. When the embolic agent was injected retrograded slowly into the gastroduodenal artery, the common hepatic artery was temporarily ligated to avoid reflux of embolic agent into the celiac trunk. Simultaneously, for the purpose of segmental embolization, we temporarily ligated right hepatic artery and this could help the rat to survive after embolization.

By the study of the imaging and pathological features, we considered the advantages of the model are: (1) We can choose the position of implantation as designed. (2) It has a high tumor uptake rate and high reproducibility of tumor growth characteristics, the procedure of implantation is simple and can be performed quickly. (3) Blood supply of the tumors mainly comes from hepatic artery and the lesions were rich in vasculature, indicating that the model is suitable for TACE experimental study. (4) The experimental methods (including tumor implantation and hepatic artery catheterization) guarantee a high post-therapy survival rate and allow the dynamic evaluation of image characteristics and treatment efficacy possible. (5) MR and CT scan can display the lesion clearly and show ascites, satellite liver nodules or lung metastasis in some models. These are helpful in animal optioning and allows noninvasive evaluation of treatment efficacy.

We conclude that the model can resemble the natural course of human HCC and have similar angiographic, CT and MR features. This tumor model has the potential to be effectively used in the experimental study of TACE.

REFERENCES

1 **Pisani P**, Parkin DM, Bray FI, Ferlay J. Estimates of the world-wide mortality from twenty-five major cancers in 1990. *Int J Cancer* 1999; **83**: 18-29

2 **Akriviadis EA**, LLovet JM, Efremidis SC, Shouval D, Canelo R, Ringes B, Meyers WC. Hepatocellualr carcinoma. *Br J Surg* 1998; **85**: 1319-1331
3 **Liu CL**, Fan ST. Nonresectional therapies for hepatocellular carcinoma. *Am J Surg* 1997; **173**: 358-365
4 **Sangro B**, Herraiz M, Martinez-Gonzalez MA, Bilbao I, Herrero I, Beloqui O, Betes M, de-la-Pena A, Cienfuegos JA, Quiroga J, Prieto J. Prognosis of hepatocellular carcinoma in relation to treatment: A multivariate analysis of 178 patients from a single European institution. *Surgery* 1998; **124**: 575-583
5 **Ueno K**, Miyazono N, Inoue H, Nishida H, Kanetsuki I, Nakajo M. Transcatheter arterial chemoembolization therapy using iodized oil for patients with unresectable hepatocellular carcinoma: evaluation of three kinds of regimens and analysis of prognostic factors. *Cancer* 2000; **88**: 1574-1581
6 **Chia-Hsien Cheng J**, Chuang VP, Cheng SH, Lin YM, Cheng TI, Yang PS, Jian JJ, You DL, Horng CF, Huang AT. Unresectable hepatocellular carcinoma treated with radiotherapy and/or chemoembolization. *Int J Cancer* 2001; **96**: 243-252
7 **Fan J**, Ten GJ, He SC, Guo JH, Yang DP, Wang GY. Arterial chemoembolization for hepatocellular carcinoma. *World J Gastroenterol* 1998; **4**: 33-37
8 **Okada S**. Transcatheter arterial embolization for advanced hepatocellular carcinoma: the controversy continues. *Hepatology* 1998; **27**: 1743-1744
9 **Yang R**, Rescorla FJ, Reilly CR, Faught PR, Sanghvi NT, Lumeng L, Franklin TD, Grosfeld JL. A reproducible rat liver cancer model for experimental therapy: introducing a technique of intrahepatic tumor implantation. *J Surg Res* 1992; **52**: 193-198
10 **Kamphorst EJ**, Bodeker H, Koroma S, Linnemann U, Berger MR. New technique for superselective arterial (chemo-) embolization of the rat liver. *Lab Anim Sci* 1999; **49**: 216-219
11 **Kamada K**, Nakanishi T, Kitamoto M, Aikata H, Kawakami Y, Ito K, Asahara T, Kajiyama G. Long-term prognosis of patients undergoing transcatheter arterial chemoembolization for unresectable hepatocellular carcinoma: comparison of cisplatin lipiodol suspension and doxorubicin hydrochloride emulsion. *J Vasc Interv Radiol* 2001; **12**: 847-854
12 **Zhang Z**, Liu Q, He J, Yang J, Yang G, Wu M. The effect of preoperative transcatheter hepatic arterial chemoembolization on disease-free survival after hepatectomy for hepatocellular carcinoma. *Cancer* 2000; **89**: 2606-2612
13 **Chen MS**, Li JQ, Zhang YQ, Lu LX, Zhang WZ, Yuan YF, Guo YP, Lin XJ, Li GH. High-dose iodized oil transcatheter arterial chemoembolization for patients with large hepatocellular carcinoma. *World J Gastroenterol* 2002; **8**: 74-78
14 **Llado L**, Virgili J, Figueras J, Valls C, Dominguez J, Rafecas A, Torras J, Fabregat J, Guardiola J, Jaurrieta E. A prognostic index of the survival of patients with unresectable hepatocellular carcinoma after transcatheter arterial chemoembolization. *Cancer* 2000; **88**: 50-57
15 **Trevisani F**, De Notariis S, Rossi C, Bernardi M. Randomized control trials on chemoembolization for hepatocellular carcinoma: is there room for new studies? *J Clin Gastroenterol* 2001; **32**: 383-389
16 **Chan AO**, Yuen MF, Hui CK, Tso WK, Lai CL. A prospective study regarding the complications of transcatheter intraarterial lipiodol chemoembolization in patients with hepatocellular carcinoma. *Cancer* 2002; **94**: 1747-1752
17 **Lee SH**, Hahn ST, Park SH. Intraarterial lidocaine administration for relief of pain resulting from transarterial chemoembolization of hepatocellular carcinoma: its effectiveness and optimal timing of administration. *Cardiovasc Intervent Radiol* 2001; **24**: 368-371
18 **Lee JK**, Chung YH, Song BC, Shin JW, Choi WB, Yang SH, Yoon HK, Sung KB, Lee YS, Suh DJ. Recurrences of hepatocellular carcinoma following initial remission by transcatheter arterial chemoembolization. *J Gastroenterol Hepatol* 2002; **17**: 52-58
19 **Caturelli E**, Siena DA, Fusilli S, Villani MR, Schiavone G, Nardella M, Balzano S, Florio F. Transcatheter arterial chemoembolization for hepatocellular carcinoma in patients with cirrhosis: evaluation of damage to nontumorous liver tissue-long-term prospective study. *Radiology* 2000; **215**: 123-128
20 **Lee HS**, Kim JS, Choi IJ, Chung JW, Park JH, Kim CY. The safety and efficacy of transcatheter arterial chemoembolization in the treatment of patients with hepatocellular carcinoma and main portal vein obstruction. A prospective controlled study. *Cancer* 1997; **79**: 2087-2094
21 **Poon RT**, Ngan H, Lo CM, Liu CL, Fan ST, Wong J. Transarterial chemoembolization for inoperable hepatocellular carcinoma and postresection intrahepatic recurrence. *J Surg Oncol* 2000; **73**: 109-114
22 **Selzner M**, Bielawska A, Morse MA, Rudiger HA, Sindram D, Hannun YA, Clavien PA. Induction of apoptotic cell death and prevention of tumor growth by ceramide analogues in metastatic human colon cancer. *Cancer Res* 2001; **61**: 1233-1240
23 **Gervaz P**, Scholl B, Padrun V, Gillet M. Growth inhibition of liver metastases by the anti-angiogenic drug TNP-470. *Liver* 2000; **20**: 108-113
24 **Shiba H**, Okamoto T, Futagawa Y, Ohashi T, Eto Y. Efficient and cancer-selective gene transfer to hepatocellular carcinoma in a rat using adenovirus vector with iodized oil esters. *Cancer Gene Ther* 2001; **8**: 713-718
25 **Tang ZY**, Sun FX, Tian J, Ye SL, Liu YK, Liu KD, Xue Q, Chen J, Xia JL, Qin LX, Sun SL, Wang L, Zhou J, Li Y, Ma ZC, Zhou XD, Wu ZQ, Lin ZY, Yang BH. Metastatic human hepatocellular carcinoma models in nude mice and cell line with metastatic potential. *World J Gastroenterol* 2001; **7**: 597-601
26 **Yang CF**, Liu J, Wasser S, Shen HM, Tan CE, Ong CN. Inhibition of ebselen on aflatoxin B (1)-induced hepatocarcinogenesis in Fischer 344 rats. *Carcinogenesis* 2000; **21**: 2237-2243
27 **Kurth S**, Bulian D, Kreft B, Riemenschneider T. Intraarterial hepatic chemotherapy with fluorouracil, fluorodeoxyuridine, mitomycin C, cisplatin or methotrexate as single-agent anticancer drugs for a transplanted experimental liver tumor in rats. *J Cancer Res Clin Oncol* 1996; **122**: 421-426
28 **Bastian P**, Bartkowski R, Kohler H, Kissel T. Chemo-embolization of experimental liver metastases. Part I: distribution of biodegradable microspheres of different sizes in an animal model for the locoregional therapy. *Eur J Pharm Biopharm* 1998; **46**:243-254
29 **Gervaz P**, Scholl B, Padrun V, Gillet M. Growth inhibition of liver metastases by the anti-angiogenic drug TNP-470. *Liver* 2000; **20**: 108-113
30 **Guo WJ**, Li J, Ling WL, Bai YR, Zhang WZ, Cheng YF, Gu WH, Zhuang JY Influence of hepatic arterial blockage on blood perfusion and VEGF, MMP-1 expression of implanted liver cancer in rats. *World J Gastroenterol* 2002; **8**: 476-479
31 **Krinsky GA**, Nguyen MT, Lee VS, Rosen RJ, Goldenberg A, Theise ND, Morgan G, Rofsky NM. Dysplastic nodules and hepatocellular carcinoma: sensitivity of digital subtraction hepatic arteriography with whole liver explant correlation. *J Comput Assist Tomogr* 2000; **24**: 628-634
32 **Chuang VP**. Hepatic tumor angiography: a subject review. *Radiology* 1983; **148**: 633-639
33 **Takayasu K**, Arii S, Matsuo N, Yoshikawa M, Ryu M, Takasaki K, Sato M, Yamanaka N, Shimamura Y, Ohto M. Comparison of CT findings with resected specimens after chemoembolization with iodized oil for hepatocellular carcinoma. *Am J Roentgenol* 2000; **175**: 699-704
34 **Vogl TJ**, Trapp M, Schroeder H, Mack M, Schuster A, Schmitt J, Neuhaus P, Felix R. Transarterial chemoembolization for hepatocellular carcinoma: volumetric and morphologic CT criteria for assessment of prognosis and therapeutic success-results from a liver transplantation center. *Radiology* 2000; **214**: 349-357
35 **De Santis M**, Alborino S, Tartoni PL, Torricelli P, Casolo A, Romagnoli R. Effects of lipiodol retention on MRI signal intensity from hepatocellular carcinoma and surrounding liver treated by chemoembolization. *Eur Radiol* 1997; **7**: 10-16
36 **Colagrande S**, Fargnoli R, Dal Pozzo F, Bindi A, Rega L, Villari N. Value of hepatic arterial phase CT versus lipiodol ultrafluid CT in the detection of hepatocellular carcinoma. *J Comput Assist Tomogr* 2000; **24**: 878-883
37 **Kubota K**, Hisa N, Nishikawa T, Fujiwara Y, Murata Y, Itoh S, Yoshida D, Yoshida S. Evaluation of hepatocellular carcinoma after treatment with transcatheter arterial chemoembolization: comparison of Lipiodol-CT, power Doppler sonography, and dynamic MRI. *Abdom Imaging* 2001; **26**: 184-190
38 **Katyal S**, Oliver JH, Peterson MS, Chang PJ, Baron RL, Carr BI. Prognostic significance of arterial phase CT for Prediction of response to transcatheter arterial chemoembolization in unresectable hepatocellular carcinoma: a retrospective analysis. *Am J Roentgenol* 2000; **175**: 1665-1672
39 **Kan Z**, Sato M, Ivancev K, Uchida B, Hedgpeth P, Lunderquist A, Rosch J, Yamada R. Distribution and effect of iodized poppyseed oil in the liver after hepatic artery embolization: experimental study in several animal species. *Radiology* 1993; **186**:861-866

Edited by Xu JY